4-17-2023

Investigating the Effect of Medium Chain Triglycerides on the Elasticity of Pulmonary Surfactant

Maksymilian Dziura
University of Windsor

Stuart R. Castillo
University of Windsor

Mitchell DiPasquale
University of Windsor

Omotayo Gbadamosi
University of Windsor

Piotr Zolnierczuk
Oak Ridge National Laboratory

See next page for additional authors

Investigating the Effect of Medium Chain Triglycerides on the Elasticity of Pulmonary Surfactant

Maksymilian Dziura,[†] Stuart R. Castillo,[‡] Mitchell DiPasquale,[‡] Omotayo Gbadamosi,[‡] Piotr Zolnierczuk,[¶] Michihiro Nagao,[§,‖,⊥] Elizabeth G. Kelley,[§] and Drew Marquardt[*,†,#]

†*Department of Chemistry and Biochemistry, University of Windsor, Windsor, ON, Canada*

‡*Department of Chemistry and Biochemistry, University of Windsor, Windsor, ON, Canada N9B 3P4*

¶*Neutron Scattering Division, Oak Ridge National Laboratory, Oak Ridge, TN 37830, United States*

§*National Institute of Standards and Technology, Center for Neutron Research, Gaithersburg, 20899, USA*

‖*University of Maryland, Department of Materials Science and Engineering, College Park, 20742, USA*

⊥*University of Delaware, Department of Physics and Astronomy, Newark, 19716, USA*

#*Department of Physics, University of Windsor, Windsor, ON, Canada*

E-mail: drew.marquardt@uwindsor.ca

Abstract

In recent years, vaping has increased in both popularity and ease of access. This has

led to an outbreak of a relatively new condition known as e-cigarette/vaping-associated lung injury (EVALI). This injury can be caused by physical interactions between the pulmonary surfactant (PS) in the lungs and toxins typically found in vaping solutions, such as medium chain triglycerides (MCT). MCT has been largely used as a carrier agent within many cannabis products commercially available on the market. Pulmonary surfactant ensures proper respiration by maintaining low surface tensions and interface stability throughout each respiratory cycle. Therefore any impediments to this system that negatively affects the efficacy of this function will have a strong hindrance on the individual's quality of life. Herein, neutron spin echo (NSE) and Langmuir trough rheology were used to probe the effects of MCT on the mechanical properties of pulmonary surfactant. Alongside a porcine surfactant extract, two lipid-only mimics of progressing complexity were used to study MCT effects in a range of systems that are representative of endogenous surfactant. MCT was shown to have a greater biophysical effect on bilayer systems compared to monolayers, which may align with biological data to propose a mechanism of surfactant inhibition by MCT oil.

Introduction

One of the most important physiological functions is respiration, governed by the expansion and compression of the lungs. Within the lungs are small sacs called alveoli, which are coated with a film of pulmonary surfactant (PS). This air-liquid interface is responsible for the efficient nature of breathing.[1] PS not only has important biophysical properties, such as reaching near-zero surface tensions which increases the pulmonary compliance, but also confers immunological capabilities to the lungs.[2]

The proper function of PS is largely reliant on its composition and the associated biomechanical features. PS is a system comprised of lipids and proteins in a 9:1 ratio, in which the diversity of lipids slightly varies from species to species.[3–6] In regards to the lipid fraction, a large portion ($\approx 80\%$) of it is primarily phosphatidylcholines (PC), with the most

abundant being 1,2-dipalmitoyl-sn-glycero-3-phosphocholine (DPPC), making up approximately 50% of PC lipids.[3] Another important class of lipids is unsaturated phospholipids, such as 1-palmitoyl-2-oleoyl-sn-glycero-3-phospho-1'-rac-glycerol (POPG), which makes up approximately 10 mol% of total lipid content. Neutral lipids, such as cholesterol, are the last major lipid class of the PS, and makes up approximately 10 mol% of the total lipid content.[7,8] Surfactant proteins (SP), consisting of SP-A, SP-B, SP-C, and SP-D also play a key role in PS functionality; hydrophilic SP-A and SP-D primarily confer an immunological role in the surfactant, whereas hydrophobic SP-B and SP-C augment important biophysical characteristics to the system.[9]

The introduction of foreign molecules into the active PS film can be detrimental to the respiration process by increasing the amount of work needed to breath.[10] Interactions between toxins and PS have been investigated in understanding the onset of e-cigarette/vaping use-associated lung injury (EVALI).[11–16] The growing popularity of inhaled aerosol devices in the market has led to an outbreak of EVALI, with the Centers for Disease Control and Prevention (CDC) reporting 2602 cases and 57 deaths within the United States as of the beginning of 2020.[17] When surveyed, most of the affected reported use of tetrahydrocannabinol (THC) containing products, which were either THC-only containing products or mixtures of THC and nicotine.[17,18] The lack of sufficient quality control and large variety of e-liquid formulations makes it difficult in understanding from where this EVALI breakout originates. There have been comprehensive studies investigating the compositions of various vaping oils using gas-chromatography mass spectrometry (GC-MS), which has given rise to many possible candidates behind the cause of EVALI.[19] Notably, many compounds such as terpenes, cannabinoids, vitamin E acetate (VEA), polyethylene glycol, and medium chain triglycerides (MCT) have been notably identified in many vaping oil cartridges.[19–21]

Of these compounds, MCT is relatively common, with data showing it being found in roughly 20% of cannabis cartridges in California, as investigated by Guo et al.[19] However, MCT has been gaining a positive reputation in the public eye as a healthy energy source

by the Food and Drug Administration (FDA) as a food additive. Conversely, the FDA has deemed MCT potentially harmful when inhaled as an aerosol.[10] MCT is composed of three fatty acid chains with each chain ranging from 6 to 12 carbons, which includes caproic acid (C6), caprylic acid (C8), capric acid (C10), and lauric acid (C12), depicted in Figure 1.[19,22] MCT are typically functionally used as a thickening agent for vaping oils to give the oil a more desirable look and aroma.[23] Studies by Guo et al. and Blount et al., have shown that MCT is present in the inhaled vapour, with trace amounts being detected in the bronchoalveolar lavage fluid of EVALI patients.[19,24] Other studies have also shown that MCT plays a role in the area of oxidative stress and inflammation within the lungs.[10,11] This indicates that MCT has the capacity to enter the respiratory system and physically interact with the pulmonary surfactant or alveolar cells. Despite this, there is limited knowledge about the exact mechanism of EVALI and other lung injuries, warranting a study of the role of MCT in disrupting pulmonary surfactant function and biophysical nature, as PS is the first hydrophobic interface to interact with the excipient.

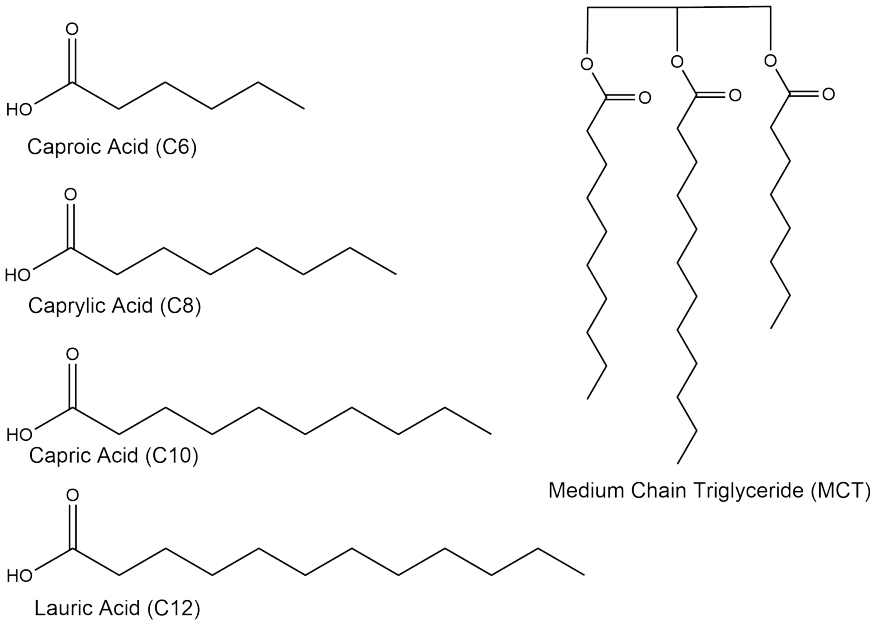

Figure 1: Medium chain triglycerides are typically made up of a combination of 3 medium chain fatty acids (C6-C12). These fatty acids can include carpoic/hexanoic acid, caprylic/octanoic acid, capric/decanoic acid, and lauric/dodecanoic acid can make up the alkyl chains of MCT

Herein, neutron spin echo spectroscopy (NSE) is employed to delve into the mechanical properties of the systems of interest. NSE is a quasi-elastic neutron scattering technique that probes the membrane dynamics at the time and length scales of thermal undulations.[25] This method has been used to investigate the dynamics and associated membrane properties of lipid vesicles by many groups.[25–30] This allows for the extraction of important information such as the effective bending modulus of PS systems which can shed light on the compressibility of the lipid environment.[25] For example, if MCT found in vaping solutions lowers the bending rigidity of PS systems, this may still permit for adsorption and respreading to occur, however it can still lead to a compromised integrity of the film at the vital near-zero surface tensions.[25]

The present study investigates the effect of MCT on the elasticity of representative PS systems. MCT oil is incorporated into mimic systems of varying complexity: a simple lipid-only system of pure DPPC, a *PS-Mimic* system comprised of the four major lipid components DPPC/POPC/POPG/Chol in a stoichiometric mixture (48/32/10/10),[25] and an animal-derived system, Curosurf, including SP-B and SP-C. Although some of these systems are protein-free, pure DPPC remains a regularly used simple replica of PS, while the *PS-Mimic* serves as a more comprehensive representation.[25,31] With mimic systems of increasing complexity, we assess the fundamental effects of MCT on surfactant elasticity.

Experimental

Materials

The synthetic lipids 1,2-dipalmitoyl-sn-glycero-3-phosphocholine [di-16:0 PC, DPPC] and 1-palmitoyl-2-oleoyl-glycero-3-phosphocholine [16:0/ 18:1 PC, POPC] were purchased from Anatrace Products (Maumee, OH). 1-palmitoyl-2-oleoyl-sn-glycero-3-phospho-(1'-rac-glycerol) (sodium salt) [16:0/18:1 PG, POPG] were purchased from Avanti Polar Lipids (Alabaster, AL). Cholesterol was purchased from Sigma-Aldrich (Oakville, ON). Curosurf, produced

by Chiesi Pharmaceuticals (Parma, Italy), was purchased from Methafarm Pharmaceutical (Brantford, ON). Medium chain triglycerides (MCT) is from Emblem Cannabis (Paris, ON). The animal-derived pulmonary surfactant extract, Curosurf, was lyophilized and reconstituted in a 2:1 ratio of HPLC-grade chloroform:methanol to form a parent stock with a final concentration of 1 mg/mL. D_2O (99.9 %) was purchased from Cambridge Isotopes (Andover, MA). All water used in experimentation was from a Milli-Q Direct Water Purification System in order to ensure ultrapure water with resistivity of 18.2 MΩ·cm.

Preparation of Large Unilamellar Vesicles for Neutron Spin Echo

The unilamellar vesicles (ULVs) for the neutron scattering experiment were prepared by carefully measuring out the desired volume of lipid stocks into glass vials using gas-tight Hamilton syringes. An MCT stock, prepared in chloroform, was used to dope the lipid samples to the desired concentration. The chloroform was evaporated to form lipid films in a vacuum-oven overnight under vacuum at 45 °C. Lipid-only pulmonary surfactant mimics were hydrated in D_2O to a final concentration of 50 mg/mL. Similarly, for the biologically-derived samples, extra precautions were undertaken to avoid denaturation of the proteins. Samples were slowly rotated on a rotary evaporator in the absence of vacuum with a 50 °C bath for 30 minutes to slowly hydrate the films. All samples were then subject to 5 freeze-thaw-vortex cycles (-80 to 50 °C) prior to extruding.

Following the freeze-thaw cycles, the samples were extruded using hand-held mini-extruders (Avanti Polar Lipids) at a temperature of 45 °C for 31 passes. Lipid-only mimics were extruded through a 100 nm pore-diameter polycarbonate filter, while biologically-derived mimics were extruded through a 400 nm pore-diameter, followed by a 100 nm pore-diameter filter. The two-step extrusion process was done to facilitate a more efficient extrusion of the delicate protein-lipid samples. Quality of the extruded vesicles was determined using dynamic light scattering on a Brookhaven B1-DNDC instrument equipped with a 637 nm incident laser and analyzed for 4 minutes at a 90° scattering angle. Protein viability was

characterized using circular dichroism.

Neutron Spin Echo Spectroscopy

The BL-15 neutron spin echo spectrometer at the Spallation Neutron Source at Oak Ridge National Laboratory (ORNL) was used.[32] Samples of interest were loaded into 4 cm by 4 cm quartz Hellma cells with a 4 mm path length for the measurement. Sample temperature was controlled by a ThermoJet ES (SP Scientific, Warminister, PA) to 37 ± 0.5 °C to mimic physiological temperature, or 45 °C was used for DPPC to be above the transition temperature of the lipid. The investigation looked at a scattering vector- (Q) range of approximately 0.04 Å^{-1} < Q < 0.1 Å^{-1} and Fourier times up to 100 ns employing neutron wavelengths of 5-8 Å and 8-11 Å. D_2O was measured under the same conditions as a background. The raw data were reduced to give the intermediate scattering function using the DrSPINE protocols described in Zolnierczuk et al.[33]

The intermediate scattering function, $\frac{S(Q,\tau)}{S(Q,0)}$, was fit as an exponential following the Zilman and Granek model for thin elastic films.[34]

The contributions from the diffusion of the vesicles was also taken into account, and the data were fit using the expression.

$$\frac{S(Q,\tau)}{S(Q,0)} \simeq e^{-DQ^2t} e^{-(\Gamma_{ZG}t)^{2/3}}, \tag{1}$$

Within this equation, D represents the Stokes-Einstein diffusion coefficient($D = \frac{k_BT}{6\pi\eta R}$) dependent on the hydrodynamic radius of the vesicle R, solvent viscosity η, absolute temperature T, and k_B as the Boltzmann constant.[25]

Further, following the work of Zilman and Granek, the relaxation rate, Γ_{ZG}, decays as a function of Q^3, where the slope of the linear regression is inversely proportional to the membrane rigidity. Further work by Watson and Brown extended the Zilman-Granek theory. Therefore NSE is able to measure the effective bending modulus, $\tilde{\kappa}$, which is related to the

intrinsic bending modulus, κ, by the expression.

$$\tilde{\kappa} = \kappa + 2d_n^2 k_m, \tag{2}$$

In Equation 2, d_n is the neutral surface which is thought to lie between the hydrophobic tails and hydrophilic headgroup, resulting in $d_n/2d_C = 0.5$; with d_C being the hydrocarbon thickness .[27] Additionally, k_m is the monolayer area compressibility modulus. This further results in the relationship between the relaxation rate and intrinsic bending modulus then becoming Equation 3.[35]

$$\frac{\Gamma_{ZG}}{Q^3} = 0.0069\sqrt{\frac{k_B T}{\kappa}}\frac{k_B T}{\eta}. \tag{3}$$

Langmuir Trough Rheology

The pulmonary surfactant systems were investigated using a KSV Nima KN2002 Langmuir-Blodgett trough (Nanoscience Instruments, Phoenix, AZ) with a total area of 24,300 mm^2. Before running samples, the trough and Delrin barriers were carefully cleaned using Alconox detergent (Alconox Inc, White Plains, NY) and anhydrous ethanol, rinsed using MilliQ water, and dried with filtered air. A platinum Wilhelmy plate (10 mm x 20 mm) was used to measure the surface pressure. The plate was flame sterilized to ensure cleanliness prior to usage. Once the equipment was cleaned the trough was filled with MilliQ water as the aqueous sub-phase. Previous studies have found little to no detectable difference between the use of ultrapure water compared to buffer systems.[31,36] The temperature of the trough was controlled to be 25 °C. Compression of the subphase was carried out to fully to assess the purity of the water as a function of surface pressure.

Once the equipment was clean and the subphase was confirmed to be clean, samples were loaded. Using a 50 μL Hamilton Syringe, 25 μL of the sample solution (1 mg/mL) was loaded carefully onto the aqueous phase, and the chloroform was allowed a total of 20 minutes to fully evaporate. MCT was doped into the model PS systems using a chloroform

stock.

Following evaporation, the monolayer was subject to compression, with all data being collected in triplicate and then averaged. When collecting the surface pressure-area isotherms, the films were compressed at a rate of 10mm/min until collapse occurred to monitor the full behaviour of the film. The values recorded were made in terms of trough area, as exact lipid content and molecular weight is difficult to determine for animal-derived samples. For oscillating experiments, the film was compressed to a specified surface pressure of 40 mN/m at 10 mm/min. This surface pressure was of interest as it is within the range of the approximate equilibrium surface pressure found in literature.[37–39] Once reached, the barriers oscillated at a frequency of 250 mHz to mimic breathing at a rate of 15 compression/expansions per minute. This data was collected for a total of 90 seconds.

The orientation of the Wilhelmy plate relative to the moving barriers produces contrasting responses to the applied compressions and expansions.[40] This uniaxial change in surface area forces measurement of the two-dimensional (2D) surface rheology to occur with the Wilhelmy plate oriented perpendicular and parallel to the barriers to assess the shear modulus (G) and dilatational modulus (E), respectively.

Shear deformations are dependent on sinusoidal strain (γ) changes, generating a response of shear stress (τ). The complex 2D shear modulus, G^*, is the cumulative shear deformation equal to the sum of the real 2D shear storage (elastic) modulus (G') and imaginary 2D shear loss (viscous) modulus (G''):[41]

$$\gamma = \gamma_0 sin(\omega t) \tag{4}$$

$$\tau = \tau_0 sin(\omega t + \delta) \tag{5}$$

$$|G^*| = \frac{\tau_0}{\gamma_0} = G' + iG'' = |G^*|cos\delta + i|G^*|sin\delta \tag{6}$$

where γ_0 is the amplitude of shear strain, τ_0 is the amplitude of shear stress, ω is the angular frequency of the oscillation, δ is the phase angle, and t is time.[41]

Dilatational 2D deformations are defined by a stress response in surface tension (σ) produced by sinusoidal changes in surface area strain (A). As in the shear modulus, the complete dilatational modulus is described by the complex 2D quantity E^*, comprised of its real and imaginary components, the 2D dilatational storage modulus (E') and the 2D dilatational loss modulus (E''), respectively. This relationship is shown below as in Rodríguez Patino et al. and Derkach et al.:

$$A = A_{surf,0} + A_0 sin(\omega t) \tag{7}$$

$$\sigma = \sigma_{surf,0} + \sigma_0 sin(\omega t + \delta) \tag{8}$$

$$E^* = \frac{d\sigma}{d\ln A} = -\frac{d\pi}{d\ln A} = E' + iE'' = |E^*|cos\delta + i|E^*|sin\delta \tag{9}$$

where $A_{surf,0}$ and $\sigma_{surf,0}$ are the surface area and surface tension of the monolayer before oscillatory deformation, respectively, and A_0 and σ_0 are the amplitudes of surface area and surface tension, respectively.[41,42]

The ratio of loss modulus to storage modulus, the loss tangent, is represented by the tangent of the phase angle, tanδ.[41] In both viscoelastic properties, the loss tangent is a relative measurement of viscous energy loss to elastic energy storage:[41]

$$tan\delta_G = \frac{G''}{G'} \quad \text{and} \quad tan\delta_E = \frac{E''}{E'} \tag{10}$$

This phase angle is also directly related to hysteresis (i.e., non-reversible behaviour) in the surface tension, which critically influences the biophysical function of PS, namely in interfacial adsorption/respreading.[3] Loss tangent values closer to 1 represent monolayers

with more fluid-like behaviour, whereas more solid-like monolayers have tanδ values closer to 0.

Results

Elastic Properties of Bilayer Systems by Neutron Spin Echo

Neutron spin echo (NSE) spectroscopy was used to probe the bilayer dynamics of the PS systems. Two lipid-only (DPPC and *PS-mimic*) and an animal-derived system (Curosurf) were investigated. Although pulmonary surfactant is most often referred to as a monolayer in its active form, bilayer structures are also found within the lungs.[43] The studied bilayer systems were doped with either 2 mol% or 10 mol% MCT to probe the effect of MCT on the bending rigidity using NSE. This technique allowed for state-of-the-art measurements of the dynamic properties on the correct time and length scale of bilayer undulations, allowing for the extraction of the effective bending modulus $\tilde{\kappa}$. These undulations were either measured at physiological temperature of 37 °C, or 45°C in the case of the DPPC samples to ensure the temperature was above the lipid melting point. This DPPC samples were also doped with 5 mol% POPG to assist with unilamellarity.[44] The intermediate scattering function, $\frac{S(Q,\tau)}{S(Q,0)}$, was fit using the Zilman-Granek model for thin elastic films.[34]

$$\frac{S(Q,\tau)}{S(Q,0)} \simeq e^{-DQ^2t} e^{-(\Gamma_{ZG}t)^{2/3}} \tag{11}$$

The resulting analysis of $\tilde{\kappa}$ shows an overall decrease of membrane rigidity with the addition of 2 mol% and 10 mol% MCT in the proteinless samples (DPPC and *PS-mimic*), as seen in Figure 2. However, for the Curosurf samples, the addition of 2 mol% shows a minimal increase in rigidity and subsequently softens with the addition of 10 mol% MCT. The relative values show an overall softening effect of the lipid-only systems, with the *PS-mimic* having a higher rigidity compared to the DPPC, which matches previous data from

our group.[25] Interestingly, the Curosurf data is the only set to show a very slight increase in rigidity with an addition of 2 mol%, however this finding is not significant. Although, this could be due to the inclusion of a greater diversity of lipids that may cause differing interactions with MCT. Furthermore, previous work has shown that membrane-associated proteins or surface active components often stiffen membranes.[45,46] The greater molecular diversity of Curosurf may also lead to a greater amount of potential interactions with the dopant, which may explain why the biologically-derived systems shows different trends than the simpler lipid-only mimics.

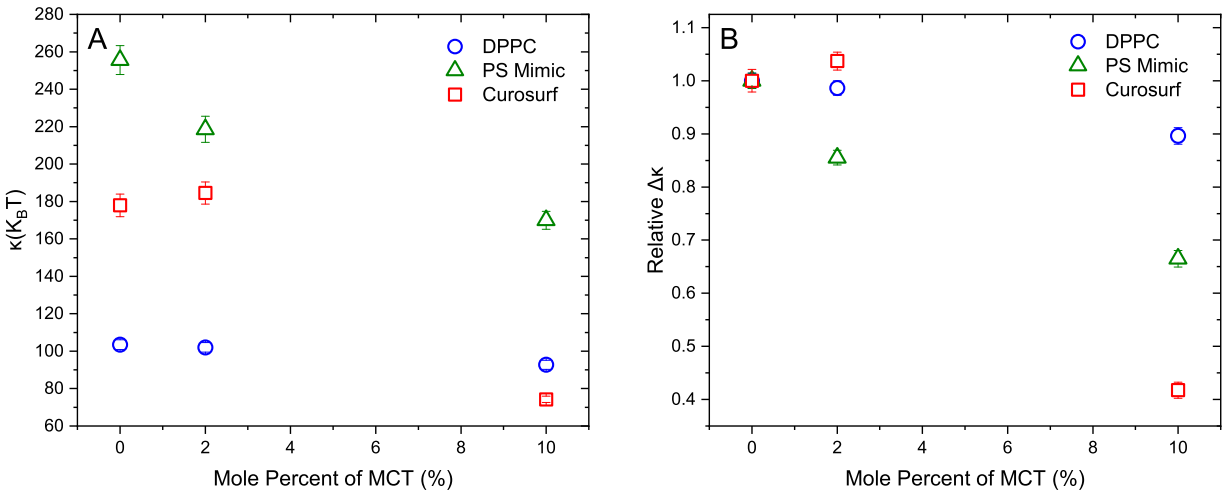

Figure 2: Experimental data extracted from neutron spin echo samples portraying the membrane rigidity. (A) $\kappa(K_BT)$ for the samples are plotted in absence of MCT, as well as 2 and 10 mol% MCT for DPPC (45 °C), *PS-mimic* (37 °C), and Curosurf samples (37 °C). (B) Normalized values of $\kappa(K_BT)$ are depicted to see a relative change in each system

Surface Pressure-Area Isotherms

The surface pressure-area isotherms were collected for all samples of interest and are shown in Figure 3. Panel A shows the isotherms of the DPPC system, with the undoped DPPC sample showing a phase profile matching that in literature.[47,48] There is a visible phase transition occurring at ≈ 5 mN/m with collapse occurring at ≈ 60 mN/m. Following the addition of MCT into the samples at 2 mol% and 10 mol%, the films collapse at a lower

surface pressure. Furthermore, the addition of 10 mol% MCT appears to change from the typical DPPC phase profile, with a less pronounced transition that the undoped and 2 mol% experience at around 5 mN/m.

Isotherms of *PS-mimic* in Panel B appear to show a brief plateau region at approximately 40 mN/m. This plateau is also characteristic of animal-derived surfactants, showing similar behaviour in both the lipid-only sample and animal-derived.[31] This region is characteristic of monolayer-to-multilayer structural rearrangement experienced by pulmonary surfactant during compression. Curosurf behaved similarly, however, the plateau region around 40 mN/m was longer and constituent, which is consistent with animal-derived surfactants in literature.[49–51] Interestingly, the *PS-mimic* is better able to accommodate the addition of MCT as all conditions collapse at approximately 57 mN/m. In comparison, undoped Curosurf experiences the highest collapse pressure in its series, with the MCT-incorporated samples collapsing at lower surface pressures. Therefore the Curosurf series, similar to the DPPC, appears to collapse at lower surface pressures when doped with MCT, which may corrupt the ability of the PS to achieve near-zero surface tension.

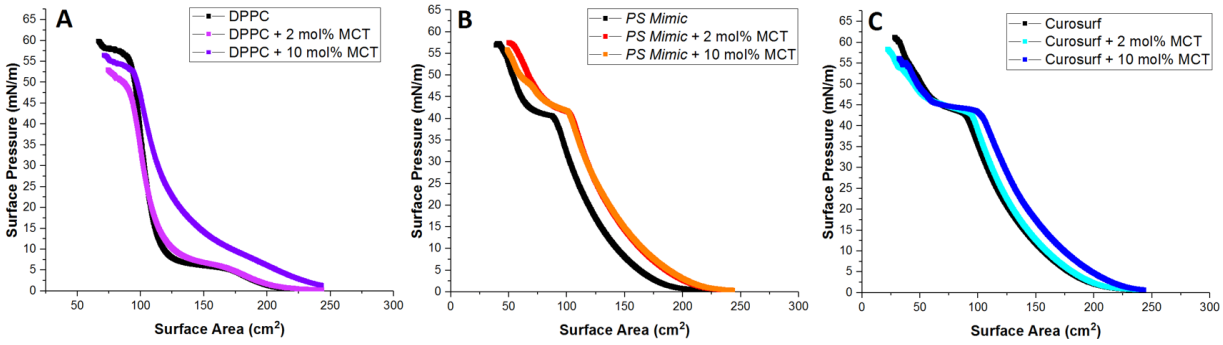

Figure 3: Langmuir surface pressure-area isotherms of DPPC (A), *PS-mimic* (B), and Curosurf (B) are shown. In each respective isotherm, the black traces are indicate the undoped sample, while the doping of 2 and 10 mol% MCT is indicated by the colour in the respective legends.

Elastic and Viscous Properties Through Oscillating Rheometry

Three systems were investigated to see how the addition of MCT affected the two-dimensional interfacial rheology through the use of the oscillating barrier method on a Langmuir trough. The Wilhelmy plate was oriented in two positions in relation to the barriers. A parallel orientation gives information on the dilatational response, while the perpendicular positioning delivers insight on the shear response.

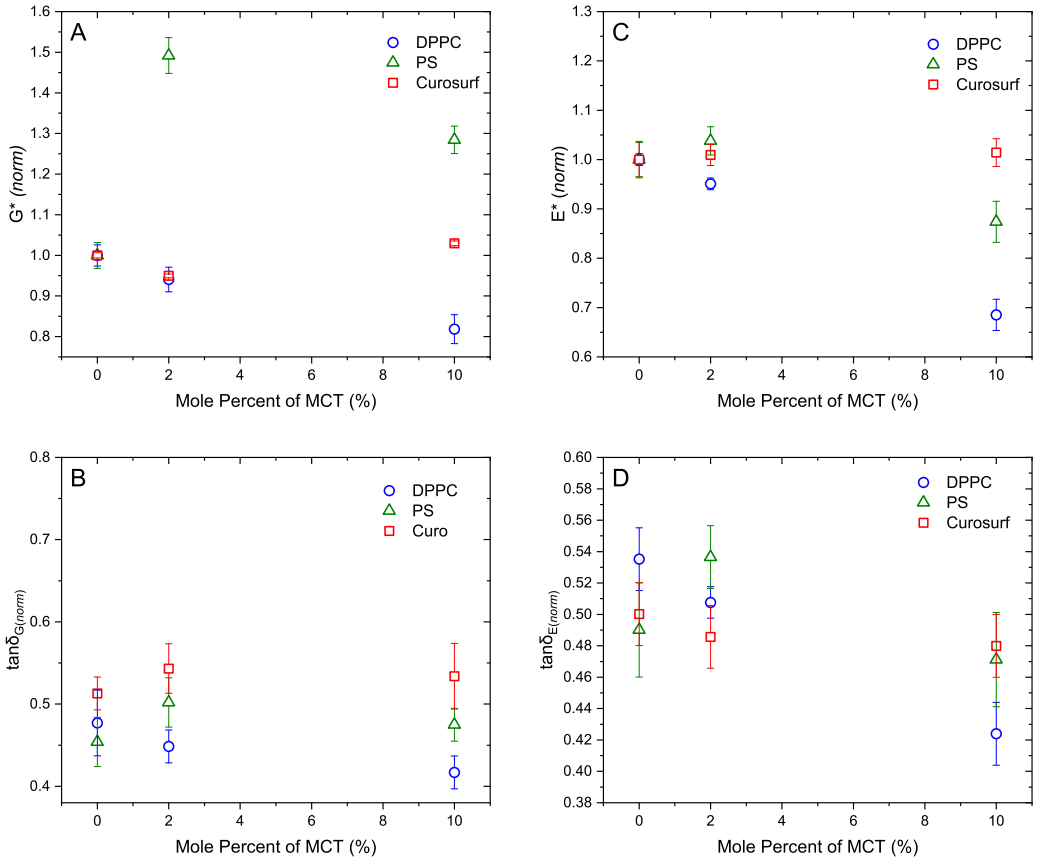

Figure 4: Normalized values of the shear and dilatational moduli (A and C) are shown from oscillatory barrier experiments. The tanδ values are also depicted (B and D) for the respective responses. All sample runs had temperature controlled at 25 °C

Information on the complex shear modulus (G^*) and the complex dilatational modulus (E^*) is presented as normalized values in Figure 4. Normalized values are used to portray the data to emphasize the relative change imparted by MCT to the PS system of interest.

In terms of G^* (Fig. 4A), the introduction of MCT had an insignificant effect on Curosurf.

Though the *PS-mimic* did not exhibit a clear trend with MCT content, this mimic system experienced an overall increase in the complex shear modulus throughout MCT addition. Meanwhile in the DPPC-only system, there is a steady decrease across 2 and 10 mol% MCT addition.

The trends in E^* shows a similar nature in terms of how the Curosurf behaves, where there is an insignificant change. In the lipid-only systems with the addition of 2 mol% MCT, the *PS-mimic* sees a slight increase, and the DPPC sees a slight decrease, both of which do not seem to be of significance. Interestingly, the addition of 10 mol% MCT results in a more significant decrease and greater relative changes in the complex dilatational modulus of DPPC (≈13%) and *PS-mimic* (≈32%) Ultimately, Curosurf seems to accommodate the addition of MCT in a better manner than the lipid-only systems at this surface pressure and are not significantly affected the biophysical characteristics of the surfactant film in question. This can possibly show that in this range where multilayer formation may occur, the addition of MCT is not detrimental to actual formation of the reservoirs.

Discussion

In a field with a great amount of uncertainty, there seems to be a consensus that a major cause behind of EVALI is due to physical interactions of chemicals with the pulmonary surfactant.[15,25] Pulmonary surfactant is responsible for respiration, the very function that keeps humans alive. A stable system is paramount to everyday life, therefore when the introduction of toxins starts to hinder this ability, there is a cause for concern and a motive to further investigate the addition of MCT in mimic lipid systems. It is important to note that the incorporation of MCT into phospholipid membranes has been previously investigated, showing a solubility of approximately 10 mol%,[52] suggesting MCT is able to incorporate into the lipid systems.

Our results investigate the effects that medium chain triglycerides impose on both mono-

layer and bilayer phospholipid systems, both of which are relevant in the pulmonary surfactant. Although generally described as a monolayer system, pulmonary surfactant also forms multilayers that are referred to as surfactant reservoirs.[38,53,54] These bilayers tend to form upon compression of the monolayer, which causes buckling of the film, leading to bilayer folds protruding into the water subphase of the air-water interface. Using NSE we are able to look at the bending modulus (κ) which sheds light on the elastic properties of the bilayer system in question.[55,56] Elastic properties have been reported to have significance in biological processes, such as budding, formation of stalks, and adsorption, all of which are relevant to the functionality of PS.[57,58]

Our results suggest that the incorporation of MCT had an overall softening effect on the lipid-only systems. This is consistent with fundamental work showing alkanes, comparable in size to the hydrocarbon chains of MCT, have an overall softening effect on DPPC vesicles.[28] This is also similar to previous data by DiPasquale et al. who found that vitamin E acetate, another compound heavily implicated with EVALI, also had a softening effect on PS mimics. Interestingly, Curosurf bilayer systems showed a slight difference in this behaviour. Upon the addition of 2 mol% MCT, there was a slight but non-significant increase in the effective bending modulus of the membrane, resulting in a stiffer bilayer, followed by a decrease at 10 mol%. This non-monotonic trend may be due to the greater complexity and variability of biomolecules in the animal-derived Curosurf, potentially differing interaction of the MCT with endogenous PS. Further measurements of a concentration series would be required to confirm if there is an overall net softening effect in all three systems. Nonetheless, the change in the elasticity of the bilayered-vesicles can be vital to the functions of PS, as it deviates from a PS schematic that has evolved into undergoing efficient respiration.

Toxins have been shown to have a variety of effects on PS functionality, such as on respreading of the reservoirs, reservoir stalk integrity, or pulmonary surfactant metabolism. Therefore one avenue in which MCT emanates an effect may be through its influence on bilayer elasticity.[25,59–62] According to the squeeze-out theory, bilayer reservoir systems allow

the monolayer to attain low surface tension. This suggests that DPPC becomes more concentrated in the locale of the monolayer while squeezing out more fluid non-DPPC species to form the aforementioned reservoirs,[63] although there is still debate to what degree the monolayer is concentrated in DPPC.[43] Ultimately DPPC creates a more condensed and ordered monolayer, while non-DPPC species make up the reservoir folds with a more fluid-like characteristic allowing for low surface tension during expiration.[31] Therefore the introduction of MCT has the potential to change the elasticity of the reservoir components thereby affecting efficiency of the respreading process upon subsequent expansion. The reservoirs are held to the system through a lipid stalk intermediate, promoted by surfactant proteins. Furthermore, MCT has the potential to affect stalk integrity, by hindering adsorption by changing the elasticity of a bilayer stalk.[64] Ultimately the incorporation of MCT may affect functions, such as respreading, which may decrease the biomechanical efficiency of PS, resulting in symptoms of respiratory distress.

Pulmonary surfactant metabolism and recycling can also be affected through the introduction of toxicants.[65] Portions of used pulmonary surfactant are recycled by type II pneumocytes.[66] In this sense, MCT can show an effect biophysically and cellularly if the MCT makes its way into the alveolar cells. Muthumalage et al. showed that MCT induced a significant amount of reactive oxygen species and inflammation in lung cells. Furthermore, they state that MCT combined with other toxins, such as vitamin E acetate, had shown the most pronounced effect.[11] This builds on the theory that EVALI may not be caused by a singular compound, but instead, be summative issue of multiple toxicants. This further shows the negative aspects of using MCT as a carrier agent in e-cigarette and vaping devices. This theory may also explain why EVALI patients who were using devices with MCT had smaller amounts of MCT found in the bronchoalveolar lavage (BAL), therefore this could be due to the compound making its way into the cellular system to transmit an unfavourable outcome.[24]

The next area of investigation was the use of a Langmuir trough to investigate the system

as a film. Use of the trough technique for the investigation of the PS has been an area of discussion. There are some intrinsic limitations, such as the study of a Langmuir film versus a Gibb's film, as shown by Xu et al.[53] However, Langmuir trough studies still provide for a valuable fundamental look into the biophysical properties of the systems of interest, specifically through surface pressure-area isotherms and oscillating barrier experiments. These experiments allow for a simple environment to mimic the expansion-compression cycles that happen in the respiratory system. Therefore, the fundamental biophysical properties with and without addition of toxin can be investigated. The use of added stress through compression of the monolayer allows for the observation of a full suite of phases changes in the film from the gaseous to fully condensed phase.

By compressing the PS films of interest, we are able to monitor the change in surface pressure of the system as a response to a decreasing surface area, producing possible deformations in the film. The surface pressure-area isotherms of the systems of interest show that in the undoped DPPC and Curosurf systems are able to reach a higher surface pressures in comparison to the doped samples which collapse at lower surface pressures. This shows that introduction of MCT in those environments negatively impacts the ability of reaching near-zero surface tensions. Interestingly, the *PS-mimic* is shown to collapse at a similar surface pressure whether doped or not. However, one possible reason for this is that the *PS-mimic* is the only system with cholesterol, as Curosurf is devoid of any neutral lipids and the DPPC sample was pure in nature. The inclusion of cholesterol can ultimately lead to an increasing of fluidity which can aid in the adsorption.[3] However the increase of fluidity can also result in the film not being able to attain as high of collapse pressure which is also seen in Figure 3, as the undoped *PS-mimic* collapses at a lower surface pressure compared to the undoped DPPC and Curosurf. This may suggest that the addition of MCT into the DPPC and Curosurf may result in premature collapse, possibly because how the alkyl chain of the MCT insert and pack in the *PS-mimic* in the presence of cholesterol.This may lead to the film not being able to accommodate the change in surface area leading to premature

collapse. Additionally the plateau region of the *PS-mimic* and Curosurf exhibit differing effects from the toxicant. The plateau occupies a large surface area range for the 2 mol% and 10 mol% MCT samples, compared to the negative control, in the Curosurf systems meaning that this is a region of high compressibility, suggesting altered lipid behaviour or orientation.[16] Due to this extended plateau region, the compression area of this region is increased which can affect the rapid lipid adsorption, that is important for maintaining equilibrium surface tension during the respiration process.[16] In contrast, it is the undoped *PS-mimic* that has a broader plateau region, compared to the doped samples, indicative of a higher compressibility. This further shows that the inclusion of cholesterol in this system may have an effect on how MCT interacts with the membrane, as excess cholesterol has been shown to promote highly compressible film characteristics which affects the ability to reach near-zero surface tensions.[16,67] There is also previous work showing that cholesterol altered the behaviour of cannabinoids in cholesterol-containing membranes, which may support the idea that cholesterol in the *PS-mimic* may be the reason why that system behaves differently to Curosurf.[68] This also suggests that cholesterol may be a molecule of interest when studying further interactions of vaping toxins.

Further results for this experiment were run with the Wilhelmy plate oriented in two directions, parallel and perpendicular to the Delrin barriers.[69] Parallel orientation would give light on dilatational properties, while perpendicular is shear. Systems were oscillated at a surface pressure of 40 mN/m which in the range of reported equilibrium surface pressure of pulmonary surfactant.[70–72] This data provides further information on how the PS responds to deformations, and the way the systems store and dissipate energy. The compression with the barriers causes deformations in the monolayer which may cause changes in the observed surface pressure of the system as a response. Interestingly, in both shear and dilatational moduli, Curosurf seems to adjust most favourably to the effect of MCT in a monolayer system, seen by the lowest changes in the doped systems compared to the pure PS monolayer. In the case of lipid-only systems, the dilatational moduli decrease with the addition of more

MCT, while the shear moduli increase with MCT addition in the *PS-mimic* and a slight decrease in DPPC. This could be due to the complexity of an animal-derived Curosurf system compared to the lipid-only counterpart. This would affect the overall organization of the systems, which may play into the effect of MCT. Bykov and Noskov suggests that the inclusion of a greater assortment of possible surface active components in Curosurf is a reason why the elastic properties of the system may vary greatly compared to a pure DPPC system.[46] Previous work also reports structural changes in compression-expansion cycles of Curosurf and DPPC, which may also factor in the overall elasticity of the film.[46] Further studies using different techniques may help further explain the exact effect MCT exerts on monolayer systems, such as the use of neutron reflectometry. However, the reported results provide evidence that MCT may impart a detrimental effect through a multilayer form, rather than directly to the monolayer at the air-liquid interface.

Ultimately these results provide new insights into how popular chemical compounds found in vaping products impart biophysical effects on PS. In the case of MCT oil, the most pronounced effect is seen in lipid bilayers, while valuable information of the PS films using Langmuir techniques to gain insight of altered behaviour upon compression of films at air-water interface. This would also lend well to previous work showing that MCT causes reactive oxygen species and inflammation in lung cells. This could be due to MCT making its way from the PS to the cells through potential mechanisms such as macrophage-mediated uptake or pulmonary surfactant recycling, which may cause negative respiratory symptoms.[66,73]

Conclusion

With the functionality of the respiratory system being a huge concern over the last century, whether it be old-fashioned cigarettes or newly emerging electronic vapes, there is an over-arching detriment to the lungs. In this work, we used NSE and Langmuir trough studies to investigate the biophysical properties, namely the elasticity, of mimic systems upon exposure to MCT oil. We observed a noticeable softening effect of MCT on bilayer systems compared

to a more ambiguous effect on monolayer films. We hypothesize that MCT oil may have a softening effect on bilayer and multilayer artifacts of PS environments leading to respiratory problems. This same trend is seen with the addition VEA, a compound heavily implicated with EVALI, showing further evidence that softening of PS may be one hint into fully understanding this disease. Ultimately there is no way of confirming the direct culprit behind EVALI at the moment; however, it is possible that MCT oil may work in conjunction with other toxins of interest leading to the detrimental lung health of e-cigarette and vape users.

Acknowledgement

This work acknowledges the support of the Natural Sciences and Engineering Research Council (NSERC) of Canada (funding reference number RGPIN-2018-04841, D.M.),; the NSERC Canadian Graduate Scholarship - Master's (CGS-M NSERC) program (M.Dz.); Canadian Graduate Scholarship - Master's (CGS-M CIHR) program (O.G.); program Ontario Graduate Scholarship (OGS) program (S.R.C); and Canadian Graduate Scholarship - Doctoral (CGS-D CIHR) program (M.Di.). Funding for this study was provided by the Lung Health Foundation through a Breathing as One Award. Neutron Facility access for the Neutron Spin Echo Spectrometer was provided by Spallation Neutron Source at Oak Ridge National Laboratory. We acknowledge funding support from WE-SPARK Health Institute (and University of Windsor). Mention of any commercial products or services does not imply approval or endorsement by NIST.

Supporting Information Available

The Supporting Information is available to all readers. Dilatational and shear rheology measurement values, circular dichroism plot, normalized intermediate scattering function for NSE, dynamic light scattering measurements, and bilayer structural parameters are included in the Supporting Information.

References

(1) Daniels, C. B.; Orgeig, S. Pulmonary surfactant: the key to the evolution of air breathing. *Physiology* **2003**, *18*, 151–157.

(2) Zuo, Y. Y.; Veldhuizen, R. A.; Neumann, A. W.; Petersen, N. O.; Possmayer, F. Current perspectives in pulmonary surfactant — Inhibition, enhancement and evaluation. *Biochimica et Biophysica Acta (BBA) - Biomembranes* **2008**, *1778*, 1947–1977.

(3) Veldhuizen, R.; Nag, K.; Orgeig, S.; Possmayer, F. The role of lipids in pulmonary surfactant. *Biochimica et Biophysica Acta (BBA)-Molecular Basis of Disease* **1998**, *1408*, 90–108.

(4) Postle, A. D.; Heeley, E. L.; Wilton, D. C. A comparison of the molecular species compositions of mammalian lung surfactant phospholipids. *Comparative Biochemistry and Physiology Part A: Molecular Integrative Physiology* **2001**, *129*, 65–73.

(5) Creuwels, L.; Van Golde, L. M. G.; Haagsman, H. P. The pulmonary surfactant system: biochemical and clinical aspects. *Lung* **1997**, *175*, 1–39.

(6) Wang, F.; Liu, J.; Zeng, H. Interactions of particulate matter and pulmonary surfactant: Implications for human health. *Advances in colloid and interface science* **2020**, *284*, 102244.

(7) Orgeig, S.; Daniels, C. B. The roles of cholesterol in pulmonary surfactant: insights from comparative and evolutionary studies. *Comparative Biochemistry and Physiology Part A: Molecular Integrative Physiology* **2001**, *129*, 75–89.

(8) Dziura, M.; Mansour, B.; DiPasquale, M.; Chandrasekera, P. C.; Gauld, J. W.; Marquardt, D. Simulated Breathing: Application of Molecular Dynamics Simulations to Pulmonary Lung Surfactant. *Symmetry* **2021**, *13*.

(9) McCormack, F. X.; Whitsett, J. A. The pulmonary collectins, SP-A and SP-D, orchestrate innate immunity in the lung. *The Journal of clinical investigation* **2002**, *109*, 707–712.

(10) Chand, H. S.; Muthumalage, T.; Maziak, W.; Rahman, I. Pulmonary toxicity and the pathophysiology of electronic cigarette, or vaping product, use associated lung injury. *Frontiers in pharmacology* **2020**, *10*, 1619.

(11) Muthumalage, T.; Lucas, J. H.; Wang, Q.; Lamb, T.; McGraw, M. D.; Rahman, I. Pulmonary toxicity and inflammatory response of vape cartridges containing medium-chain triglycerides oil and vitamin E acetate: implications in the pathogenesis of EVALI. *Toxics* **2020**, *8*, 46.

(12) Graham, E.; McCaig, L.; Shui-Kei Lau, G.; Tejura, A.; Cao, A.; Zuo, Y. Y.; Veldhuizen, R. E-cigarette aerosol exposure of pulmonary surfactant impairs its surface tension reducing function. *Plos one* **2022**, *17*, e0272475.

(13) Davies, M. J.; Birkett, J. W.; Kotwa, M.; Tomlinson, L.; Woldetinsae, R. The impact of cigarette/e-cigarette vapour on simulated pulmonary surfactant monolayers under physiologically relevant conditions. *Surface and Interface Analysis* **2017**, *49*, 654–665.

(14) Sosnowski, T. R.; Jabłczyńska, K.; Odziomek, M.; Schlage, W. K.; Kuczaj, A. K. Physicochemical studies of direct interactions between lung surfactant and components of electronic cigarettes liquid mixtures. *Inhalation toxicology* **2018**, *30*, 159–168.

(15) Hayeck, N.; Zoghzoghi, C.; Karam, E.; Salman, R.; Karaoghlanian, N.; Shihadeh, A.; Eissenberg, T.; Zein El Dine, S.; Saliba, N. A. Carrier solvents of electronic nicotine delivery systems alter pulmonary surfactant. *Chemical research in toxicology* **2021**, *34*, 1572–1577.

(16) van Bavel, N.; Lai, P.; Loebenberg, R.; Prenner, E. J. Vaping additives negatively

impact the stability and lateral film organization of lung surfactant model systems. *Nanomedicine* **2022**,

(17) King, B. A.; Jones, C. M.; Baldwin, G. T.; Briss, P. A. The EVALI and youth vaping epidemics—implications for public health. *New England Journal of Medicine* **2020**, *382*, 689–691.

(18) Lu, S. J.; Li, L.; Duffy, B. C.; Dittmar, M. A.; Durocher, L. A.; Panawennage, D.; Delaney-Baldwin, E. R.; Spink, D. C. Investigation of vaping fluids recovered from New York State e-cigarette or vaping product use-associated lung injury patients. *Frontiers in chemistry* **2021**, *9*.

(19) Guo, W.; Vrdoljak, G.; Liao, V.-C.; Moezzi, B. Major constituents of cannabis vape oil liquid, vapor and aerosol in california vape oil cartridge samples. *Frontiers in Chemistry* **2021**, *9*.

(20) Smith, M. L.; Gotway, M. B.; Crotty Alexander, L. E.; Hariri, L. P. Vaping-related lung injury. *Virchows Archiv* **2021**, *478*, 81–88.

(21) Jiang, H.; Ahmed, C. M. S.; Martin, T. J.; Canchola, A.; Oswald, I. W. H.; Garcia, J. A.; Chen, J. Y.; Koby, K. A.; Buchanan, A. J.; Zhao, Z. Chemical and toxicological characterization of vaping emission products from commonly used vape juice diluents. *Chemical Research in Toxicology* **2020**, *33*, 2157–2163.

(22) Cassiday, L. Coconut oil boom. *INFORM: International News on Fats, Oils, and Related Materials* **2016**, *27*, 6–13.

(23) Cowan, E. A.; Tran, H.; Gray, N.; Perez, J. J.; Watson, C.; Blount, B. C.; Valentín-Blasini, L. A gas chromatography-mass spectrometry method for quantifying squalane and squalene in aerosol emissions of electronic cigarette, or vaping, products. *Talanta* **2022**, *238*, 122985.

(24) Blount, B. C.; Karwowski, M. P.; Morel-Espinosa, M.; Rees, J.; Sosnoff, C.; Cowan, E.; Gardner, M.; Wang, L.; Valentin-Blasini, L.; Silva, L. Evaluation of bronchoalveolar lavage fluid from patients in an outbreak of e-cigarette, or vaping, product use–associated lung injury—10 states, August–October 2019. *Morbidity and Mortality Weekly Report* **2019**, *68*, 1040.

(25) DiPasquale, M.; Gbadamosi, O.; Nguyen, M. H. L.; Castillo, S. R.; Rickeard, B. W.; Kelley, E. G.; Nagao, M.; Marquardt, D. A mechanical mechanism for vitamin e acetate in E-cigarette/Vaping-Associated lung injury. *Chemical research in toxicology* **2020**, *33*, 2432–2440.

(26) Castillo, S. R.; Rickeard, B. W.; DiPasquale, M.; Nguyen, M. H. L.; Lewis-Laurent, A.; Doktorova, M.; Kav, B.; Miettinen, M. S.; Nagao, M.; Kelley, E. G. Probing the Link between Pancratistatin and Mitochondrial Apoptosis through Changes in the Membrane Dynamics on the Nanoscale. *Molecular Pharmaceutics* **2022**, *19*, 1839–1852.

(27) Nagao, M.; Kelley, E. G.; Ashkar, R.; Bradbury, R.; Butler, P. D. Probing elastic and viscous properties of phospholipid bilayers using neutron spin echo spectroscopy. *The journal of physical chemistry letters* **2017**, *8*, 4679–4684.

(28) Usuda, H.; Hishida, M.; Kelley, E. G.; Yamamura, Y.; Nagao, M.; Saito, K. Interleaflet coupling of n-alkane incorporated bilayers. *Physical Chemistry Chemical Physics* **2020**, *22*, 5418–5426.

(29) Sharma, V.; Mamontov, E. Multiscale lipid membrane dynamics as revealed by neutron spectroscopy. *Progress in Lipid Research* **2022**, 101179.

(30) Gupta, S.; Ashkar, R. The dynamic face of lipid membranes. *Soft Matter* **2021**, *17*, 6910–6928.

(31) Zhang, H.; Fan, Q.; Wang, Y. E.; Neal, C. R.; Zuo, Y. Y. Comparative study of clinical

pulmonary surfactants using atomic force microscopy. *Biochimica et Biophysica Acta (BBA)-Biomembranes* **2011**, *1808*, 1832–1842.

(32) Ohl, M.; Monkenbusch, M.; Arend, N.; Kozielewski, T.; Vehres, G.; Tiemann, C.; Butzek, M.; Soltner, H.; Giesen, U.; Achten, R. The spin-echo spectrometer at the Spallation Neutron Source (SNS). *Nuclear Instruments and Methods in Physics Research Section A: Accelerators, Spectrometers, Detectors and Associated Equipment* **2012**, *696*, 85–99.

(33) Zolnierczuk, P. A.; Holderer, O.; Pasini, S.; Kozielewski, T.; Stingaciu, L. R.; Monkenbusch, M. Efficient data extraction from neutron time-of-flight spin-echo raw data. *Journal of applied crystallography* **2019**, *52*, 1022–1034.

(34) Zilman, A. G.; Granek, R. Undulations and dynamic structure factor of membranes. *Physical review letters* **1996**, *77*, 4788.

(35) Watson, M. C.; Brown, F. L. H. Interpreting membrane scattering experiments at the mesoscale: the contribution of dissipation within the bilayer. *Biophysical journal* **2010**, *98*, L9–L11.

(36) Zuo, Y. Y.; Tadayyon, S. M.; Keating, E.; Zhao, L.; Veldhuizen, R. A.; Petersen, N. O.; Amrein, M. W.; Possmayer, F. Atomic force microscopy studies of functional and dysfunctional pulmonary surfactant films, II: albumin-inhibited pulmonary surfactant films and the effect of SP-A. *Biophysical Journal* **2008**, *95*, 2779–2791.

(37) Keating, E.; Zuo, Y. Y.; Tadayyon, S. M.; Petersen, N. O.; Possmayer, F.; Veldhuizen, R. A. A modified squeeze-out mechanism for generating high surface pressures with pulmonary surfactant. *Biochimica et Biophysica Acta (BBA)-Biomembranes* **2012**, *1818*, 1225–1234.

(38) Amrein, M.; Von Nahmen, A.; Sieber, M. A scanning force-and fluorescence light mi-

croscopy study of the structure and function of a model pulmonary surfactant. *European biophysics journal* **1997**, *26*, 349–357.

(39) Casals, C.; Cañadas, O. Role of lipid ordered/disordered phase coexistence in pulmonary surfactant function. *Biochimica et Biophysica Acta (BBA)-Biomembranes* **2012**, *1818*, 2550–2562.

(40) Petkov, J. T.; Gurkov, T. D.; Campbell, B. E.; Borwankar, R. P. Dilational and Shear Elasticity of Gel-like Protein Layers on Air/Water Interface. *Langmuir* **2000**, *16*, 3703–3711.

(41) Derkach, S. R.; Krägel, J.; Miller, R. Methods of Measuring Rheological Properties of Interfacial Layers (Experimental Methods of 2D Rheology). *Colloid Journal* **2008**, *71*, 1–17.

(42) Rodríguez Patino, J. M.; Sánchex, C. C.; Rodríguez Niño, M. R.; Fernándex, M. C. Structural-Dilational Characteristics Relationships of Monoglyceride Monolayers at the Air-Water Interface. *Langmuir* **2001**, *17*, 4003–4013.

(43) Yu, S.-H.; Possmayer, F. Lipid compositional analysis of pulmonary surfactant monolayers and monolayer-associated reservoirs. *Journal of lipid research* **2003**, *44*, 621–629.

(44) Scott, H. L.; Skinkle, A.; Kelley, E. G.; Waxham, M. N.; Levental, I.; Heberle, F. A. On the mechanism of bilayer separation by extrusion, or why your LUVs are not really unilamellar. *Biophysical journal* **2019**, *117*, 1381–1386.

(45) Kelley, E. G.; Butler, P. D.; Nagao, M. Collective dynamics in lipid membranes containing transmembrane peptides. *Soft Matter* **2021**, *17*, 5671–5681.

(46) Bykov, A. G.; Noskov, B. A. Surface dilatational elasticity of pulmonary surfactant solutions in a wide range of surface tensions. *Colloid Journal* **2018**, *80*, 467–473.

(47) Terakosolphan, W.; Trick, J. L.; Royall, P. G.; Rogers, S. E.; Lamberti, O.; Lorenz, C. D.; Forbes, B.; Harvey, R. D. Glycerol solvates DPPC headgroups and localizes in the interfacial regions of model pulmonary interfaces altering bilayer structure. *Langmuir* **2018**, *34*, 6941–6954.

(48) Wüstneck, R.; Perez-Gil, J.; Wüstneck, N.; Cruz, A.; Fainerman, V.; Pison, U. Interfacial properties of pulmonary surfactant layers. *Advances in colloid and interface science* **2005**, *117*, 33–58.

(49) Jiao, X.; Keating, E.; Tadayyon, S.; Possmayer, F.; Zuo, Y. Y.; Veldhuizen, R. A. Atomic force microscopy analysis of rat pulmonary surfactant films. *Biophysical Chemistry* **2011**, *158*, 119–125.

(50) Pinheiro, M.; Giner-Casares, J. J.; Lúcio, M.; Caio, J. M.; Moiteiro, C.; Lima, J. L.; Reis, S.; Camacho, L. Interplay of mycolic acids, antimycobacterial compounds and pulmonary surfactant membrane: A biophysical approach to disease. *Biochimica et Biophysica Acta (BBA)-Biomembranes* **2013**, *1828*, 896–905.

(51) Zhang, H.; Wang, Y. E.; Neal, C. R.; Zuo, Y. Y. Differential effects of cholesterol and budesonide on biophysical properties of clinical surfactant. *Pediatric research* **2012**, *71*, 316–323.

(52) Hamilton, J. A.; Vural, J. M.; Carpentier, Y. A.; Deckelbaum, R. J. Incorporation of medium chain triacylglycerols into phospholipid bilayers: effect of long chain triacylglycerols, cholesterol, and cholesteryl esters. *Journal of lipid research* **1996**, *37*, 773–782.

(53) Xu, L.; Yang, Y.; Zuo, Y. Y. Atomic force microscopy imaging of adsorbed pulmonary surfactant films. *Biophysical Journal* **2020**, *119*, 756–766.

(54) Bachofen, H.; Gerber, U.; Gehr, P.; Amrein, M.; Schürch, S. Structures of pulmonary

surfactant films adsorbed to an air–liquid interface in vitro. *Biochimica et Biophysica Acta (BBA)-Biomembranes* **2005**, *1720*, 59–72.

(55) Mell, M.; Moleiro, L. H.; Hertle, Y.; Fouquet, P.; Schweins, R.; López-Montero, I.; Hellweg, T.; Monroy, F. Bending stiffness of biological membranes: What can be measured by neutron spin echo? *The European Physical Journal E* **2013**, *36*, 1–13.

(56) Castillo, S. R.; Rickeard, B. W.; DiPasquale, M.; Nguyen, M. H. L.; Lewis-Laurent, A.; Doktorova, M.; Kav, B.; Miettinen, M. S.; Nagao, M.; Kelley, E. G.; Marquardt, D. Probing the Link between Pancratistatin and Mitochondrial Apoptosis through Changes in the Membrane Dynamics on the Nanoscale. *Molecular Pharmaceutics* **2022**, *19*, 1839–1852, PMID: 35559658.

(57) Hoffmann, I.; Michel, R.; Sharp, M.; Holderer, O.; Appavou, M.-S.; Polzer, F.; Farago, B.; Gradzielski, M. Softening of phospholipid membranes by the adhesion of silica nanoparticles–as seen by neutron spin-echo (NSE). *Nanoscale* **2014**, *6*, 6945–6952.

(58) Pérez-Gil, J. Structure of pulmonary surfactant membranes and films: the role of proteins and lipid–protein interactions. *Biochimica et Biophysica Acta (BBA)-Biomembranes* **2008**, *1778*, 1676–1695.

(59) Guzmán, E.; Santini, E. Lung surfactant-particles at fluid interfaces for toxicity assessments. *Current opinion in colloid interface science* **2019**, *39*, 24–39.

(60) Przybyla, R. J.; Wright, J.; Parthiban, R.; Nazemidashtarjandi, S.; Kaya, S.; Farnoud, A. M. Electronic cigarette vapor alters the lateral structure but not tensiometric properties of calf lung surfactant. *Respiratory Research* **2017**, *18*, 1–13.

(61) Cecchini, M. J.; Mukhopadhyay, S.; Arrossi, A. V.; Beasley, M. B.; Butt, Y. M.; Jones, K. D.; Pambuccian, S.; Mehrad, M.; Monaco, S. E.; Saqi, A. E-cigarette or vaping product use-associated lung injury: A review for pathologists. *Archives of Pathology Laboratory Medicine* **2020**, *144*, 1490–1500.

(62) Martinez-Calle, M.; Prieto, M.; Olmeda, B.; Fedorov, A.; Loura, L. M. S.; Pérez-Gil, J. Pulmonary surfactant protein SP-B nanorings induce the multilamellar organization of surfactant complexes. *Biochimica et Biophysica Acta (BBA)-Biomembranes* **2020**, *1862*, 183216.

(63) Veldhuizen, E. J. A.; Haagsman, H. P. Role of pulmonary surfactant components in surface film formation and dynamics. *Biochimica et Biophysica Acta (BBA)-Biomembranes* **2000**, *1467*, 255–270.

(64) Kozlovsky, Y.; Kozlov, M. M. Stalk model of membrane fusion: solution of energy crisis. *Biophysical journal* **2002**, *82*, 882–895.

(65) Matsumoto, S.; Fang, X.; Traber, M. G.; Jones, K. D.; Langelier, C.; Hayakawa Serpa, P.; Calfee, C. S.; Matthay, M. A.; Gotts, J. E. Dose-dependent pulmonary toxicity of aerosolized vitamin E acetate. *American journal of respiratory cell and molecular biology* **2020**, *63*, 748–757.

(66) Olmeda, B.; Martínez-Calle, M.; Pérez-Gil, J. Pulmonary surfactant metabolism in the alveolar airspace: Biogenesis, extracellular conversions, recycling. *Annals of Anatomy-Anatomischer Anzeiger* **2017**, *209*, 78–92.

(67) Gunasekara, L.; Schürch, S.; Schoel, W. M.; Nag, K.; Leonenko, Z.; Haufs, M.; Amrein, M. Pulmonary surfactant function is abolished by an elevated proportion of cholesterol. *Biochimica et Biophysica Acta (BBA)-Molecular and Cell Biology of Lipids* **2005**, *1737*, 27–35.

(68) Mavromoustakos, T.; Daliani, I. Effects of cannabinoids in membrane bilayers containing cholesterol. *Biochimica et Biophysica Acta (BBA)-Biomembranes* **1999**, *1420*, 252–265.

(69) Aumaitre, E.; Vella, D.; Cicuta, P. On the measurement of the surface pressure in Langmuir films with finite shear elasticity. *Soft Matter* **2011**, *7*, 2530–2537.

(70) Crane, J. M.; Hall, S. B. Rapid compression transforms interfacial monolayers of pulmonary surfactant. *Biophysical journal* **2001**, *80*, 1863–1872.

(71) Hawgood, S. Pulmonary surfactant apoproteins: a review of protein and genomic structure. *American Journal of Physiology-Lung Cellular and Molecular Physiology* **1989**, *257*, L13–L22.

(72) Taeusch, H. W.; De La Serna, J. B.; Perez-Gil, J.; Alonso, C.; Zasadzinski, J. A. Inactivation of pulmonary surfactant due to serum-inhibited adsorption and reversal by hydrophilic polymers: experimental. *Biophysical journal* **2005**, *89*, 1769–1779.

(73) Ghosh, A.; Ahmad, S.; Coakley, R. D.; Sassano, M. F.; Alexis, N. E.; Tarran, R. Lipid-laden macrophages are not unique to patients with E-cigarette or vaping product use–associated lung injury. *American journal of respiratory and critical care medicine* **2021**, *203*, 1030–1033.

TOC Graphic

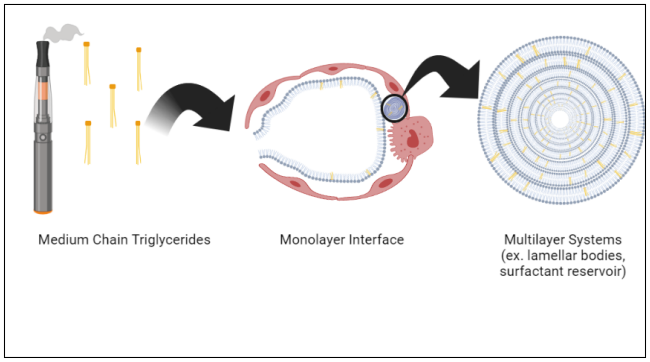
Medium Chain Triglycerides
Monolayer Interface
Multilayer Systems
(ex. lamellar bodies,
surfactant reservoir)